Geotechnical Characterization of Underground Mine Excavations from UAV-Captured Photogrammetric & Thermal Imagery

Turner, R.M.
Barrick Golden Sunlight Mine, Whitehall, MT, USA

Bhagwat, N.P., Galayda, L.J., Knoll, C.S., Russell, E.A., MacLaughlin, M.M.
Montana Tech of the University of Montana, Butte, MT, USA

ABSTRACT: Geotechnical characterization of rock masses in underground mines often involves physical measurements in supported excavations. However, unsupported stopes and drifts prevent safe access for mapping by geotechnical personnel. The advent of inexpensive, open platform unmanned aerial vehicles (UAVs) allows geotechnical personnel to characterize hazardous rock masses by utilizing traditional photogrammetric and FLIR (forward looking infrared) imagery techniques. The photogrammetric imagery can be used to capture geological structural data from the rock mass for kinematic and numerical analyses, as well as for generating geological models. In particular, the FLIR imagery has the potential to assist in identifying areas of loose rock, which typically goes unnoticed until it becomes a hazard. This paper summarizes the results of a study involving UAV flights underground at the Barrick Golden Sunlight Mine, the generation of 3D models from UAV-captured imagery, and the identification of geological data from photogrammetry models. Results confirm that the combination of off-the-shelf technologies used in this study can be successfully employed as a geotechnical tool in the underground mining environment.

1. INTRODUCTION

With the ability to fly in and out of hazardous areas while carrying a payload of instruments, unmanned aerial vehicles (UAVs) have the potential to become a versatile tool for engineers and geologists in underground mining. UAVs have become common tools in mining, but they have yet to be fully utilized in the underground environment. Surface mining operations have a variety of UAV platforms, on-board instruments, GPS devices, and dedicated software to choose from for the support of surveying, monitoring, and geological/geotechnical mapping (Knight, 2016). However, there are few UAVs and instruments that are dedicated to the underground environment, which typically has low-visibility conditions, confined openings, magnetic interference, and a lack of GPS coverage. Though not intended for operating in these conditions, off-the-shelf technology in the form of open-platform UAVs, high-resolution cameras, LED lighting, and streamlined photogrammetry software potentially allows users to capture useful information in areas not safely accessed by mine personnel. The overall goal of this research was to demonstrate that off-the-shelf technology could be used to capture high quality data that for geotechnical analyses. The components of this geotechnical tool involve obstacle detection, lighting, thermal imagery, and software.

Thermal cameras are another tool not fully utilized in the underground mining environment, but with decreasing costs and improving resolution, they can now be readily used for enhancing safety. In a rock mass containing loose ground, dilation along geologic structures or fractures within the rock mass allows the material to deform and allows infiltration of air behind the loose blocks that can be warmer or cooler than the rock mass, producing temperature contrasts between the intact rock mass and loose blocks. Consequently, these temperature contrasts can be used to infer the stability of the underground opening. Use of thermal cameras to determine the location of loose ground has been successfully demonstrated in mines with varying ambient rock mass temperatures in the United States (Iverson and Signer, 2014). It was the intent of this project to evaluate whether thermal cameras deployed on UAVs could successfully be used to detect loose blocks in inaccessible areas underground.

2. SITE CONDITIONS

The underground mining environment can be harsh on people and equipment, and open stopes likely represent the harshest setting due to the frequency of ground fall and the lack of safe accessibility to the opening. Stopes are the open spaces left behind after ore is extracted from the rock mass, and they remain open when the rock mass is sufficiently strong to stand up without artificial ground

support. However, due to the blasting used to fragment the ore, the rock mass adjacent to the stope is often highly disturbed and prone to releasing wedges and rock fall into the opening. At many underground mines, personnel are forbidden to enter stopes due to insufficient ground support and the high frequency of rock fall. For UAVs, the risk of operating in stopes is compounded by dusty, humid conditions and the lack of GPS coverage and adequate lighting. Flying within line-of-sight is both necessary and difficult underground due to sharp corners that block radio and wireless transmissions. UAVs that crash or fail while flying inside of a stope are unlikely to be recovered.

As part of this research project, UAVs were flown in underground drifts and stopes at the Barrick Golden Sunlight Mine, an underground gold mine in Whitehall, MT. Long hole stoping is used to recover ore, which leaves openings with dimensions as large as 30 m (100 ft.) wide, 60 m (200 ft.) tall, and 60 m (200 ft.) long. Stopes at the Golden Sunlight Mine typically have 2-3 access points with elevations near the bottom, middle, and top of the opening. Figure 1 shows a cross-section of the NEV stope, which is a stope mined from three draw points at the lowest access level. This stope is hosted within a thickly-bedded sandstone that is easily disturbed by blasting, and rock fall is common within the stope. This stope was flown in as part of this research because it is accessible and represents a typical stope at Golden Sunlight.
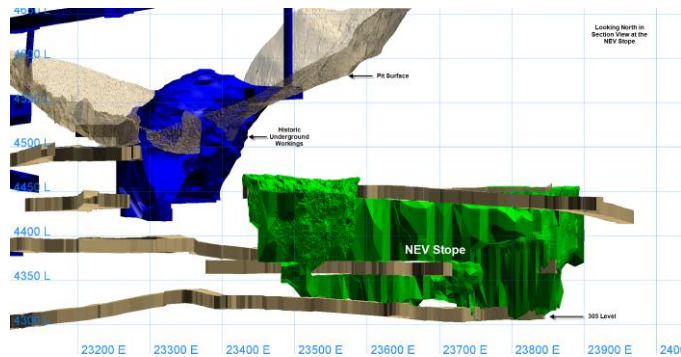

Fig. 1. Cross-section view looking north at the NEV Stope at the Barrick Golden Sunlight Mine, in Maptek Vulcan. The mine grid is in units of feet.

3. UAV AND INSTRUMENTATION

A DJI Matrice 100 (M100) UAV (shown in Figure 2) was selected to serve as the primary flying platform for this experiment because it is categorized as a research-oriented UAV with significant instrument compatibility. It is the sole DJI aircraft that is compatible with the DJI "Guidance" proximity sensing system, which is offered as an accessory to the aircraft. For this research, the M100's payload included the DJI Guidance system, an advanced flight battery (TB48D), one imaging device (either a Zenmuse X3 digital camera or a Zenmuse XT thermal camera), two Stratus LEDs ARM lights, and a LIPO

battery to power the lights. The M100 has a stated maximum takeoff mass of 3600 grams (DJI, March 2016), but the UAV was typically flown in excess of this (Table 1) for a maximum flight time of 10 minutes. This was necessary due to the weight of the lighting system (Stratus LEDs), which was the only tested lighting system able to provide sufficient illumination for photography and the Guidance system.

Fig. 2. The M100 underground at the Barrick Golden Sunlight Mine with a standard payload of lights, a camera, and the Guidance system.

Table 1. Measured masses of equipment used in this experiment. The UAV was flown with a single imaging device (either the Zenmuse X3 camera, or the Zenmuse XT camera, not both at the same time).

Instrument	Quantity	Mass (g)
M100	1	1754
TB48D Battery	1	677
Propellers	4	72
Guidance	1	337
Zenmuse X3 (XT) Camera	1	221 (270)
Stratus LED ARM LEDs	2	323
6S 3000mAh 25C LIPO Battery	1	380
Total payload with Zenmuse X3 (XT)		3764 (3813)

A DJI Zenmuse X3 camera was used in conjunction with the M100 to capture both still and video digital imagery. The Zenmuse X3, X5 and Z3 from DJI are compatible with the M100, but the Zenmuse X3 was found to have a sufficient sensor size (CMOS 1/2.3"), a larger FOV (field of view) and is the least expensive. The camera utilizes a micro SD card for local storage of high resolution imagery, while a live feed from the camera is shown in the DJI Go app at 720p (DJI, March 2016).

To capture the thermal imagery, several radiometric FLIR devices were evaluated. The radiometric devices provide thermal data for each pixel in the image, as opposed to the much lower cost non-radiometric devices that provide quantitative thermal data only for the center pixel in the image. A FLIR C3 thermal camera was initially tested

underground due to its low cost (less than $500 educational price) that was attractive for use in a high-risk environment in which the instrument can easily be lost. Although it is a useful camera for learning about thermal imagery and can detect thermal contrasts in rock masses when they exceed 0.1°C (Table 2), unfortunately, the low resolution (80 x 60 pixels) and the relatively shallow depth of field of the images made the generation of photogrammetric models difficult. Also, there are no readily available gimbals (devices that attach the instrument to the UAV) for the C3, and the lack of video recording makes using this camera difficult on a UAV (FLIR, 2016).

Research-quality thermal imagery was captured in drifts and stopes underground using the DJI Zenmuse XT thermal camera flown on the M100. This camera is integrated with a 3-axis gimbal and can be used on a variety of DJI UAVs (DJI, May 2016). Due to the relatively short distances anticipated between the camera and the walls of the stopes, a 9 mm lens was selected because it provided the widest field of view and higher magnification than provided by other lens choices. Although the cost was more than twice as high, the high-resolution version of the camera (640 pixels x 512 pixels) was selected over the low resolution version (336 pixels x 256 pixels) because it would provide the highest quality data. Table 2 contains a summary of the relevant properties of the different cameras used in this study.

Table 2. Comparison of the different cameras used.

Property	Zenmuse X3	FLIR C3	Zenmuse XT
Mass	221 g	130 g	170 g
Resolution (pixels)	4000 X 3000	80 X 60	640 X 512
Video resolution (pixels)	4096 X 2160	N/A	640 X 512
Sensor	CMOS 1/2.3"	Uncooled micro bolometer	Uncooled VOx micro bolometer
FOV	94°	41° X 31°	69° X 56°
Accuracy	N/A	± 2°C	± 4°C
Sensitivity (NEdT)	N/A	0.1°C	0.05°C
Spectral range	N/A	7.5-14 μm	7.5-13.5 μm
Radiometric	N/A	Yes	Yes

4. OBSTACLE DETECTION

The DJI Guidance system was selected for this experiment, because it is offered as an off-the-shelf obstacle detection system that allows the DJI M100 to fly indoors and in GPS-denied areas. The Guidance utilizes stereo camera pairs (the visual positioning system, or VPS) and ultrasonic sensors on five sides of the aircraft (typically each of the four sides and the bottom) to navigate and detect obstacles. Figure 3 contains a photo

of the M100 hovering with control underground. With the aid of on-board lighting, the Guidance system is detecting the ground surface and using it as a reference for remaining stationary in mid-air. Without illumination, the Guidance would not detect the ground, and the M100 would drift if not controlled by the pilot.

Fig. 3. The M100 hovering within the 895-102 intersection at the Barrick Golden Sunlight Mine. The UAV is approximately 2.75 m (9 ft.) off of the sill, and the blue light indicates that the downward-facing Guidance sensor is functioning properly and positioning the aircraft.

The most critical challenge encountered during this research project was learning how to configure and use the DJI Guidance system properly. The role of the Guidance system is to detect obstacles and prevent the UAV from flying within a specified distance of the obstacles. The documentation provided for the Guidance system is sparse and trial and error are required to configure it properly. When not configured correctly, the Guidance system failed to detect obstacles, allowing the M100 to contact the obstacles and potentially crash. Individual sensors on the system are calibrated using a computer monitor and the DJI Guidance Assistant software (DJI, 2015). It was found that if the computer monitor was too small or had low resolution, the calibration would fail. According to the available documentation, the Guidance can be mounted above or below the main platform of the M100, but in tests conducted for this project, it only functioned properly

when positioned below. The suspected reason for this is that when the Guidance sensors are positioned on top of the aircraft, the movement of the propellers (which are also positioned above the main platform) interferes with the operation of the sensors. Use of the advanced flight battery (TB48D) for the M100 allowed for the distances to obstacles to be displayed in the DJI Go app, while this was not available with the standard flight battery (TB47D). Also, it was determined that the Guidance worked properly when the Zenmuse X3 camera was attached to the M100 and did not work at all when the camera was detached. None of these observations are addressed in the documentation. It is recommended that indoor flight testing with the Guidance be conducted in a controlled environment before use underground where recovery can be difficult.

5. LIGHTING

The M100 was required to have on-board lighting to support the use of both the digital camera used for capturing imagery and the DJI Guidance proximity sensing system. It was necessary that the on-board lighting provided sufficient illumination for photogrammetry, but not so much that photos were overexposed. The lighting system also had to provide at least 10 lux (lumens per square meter) for the Guidance visual positioning system (VPS) to detect obstacles underground. Several different lighting systems were evaluated in terms of weight (battery + LEDs), lumens, beam width, and mounting options. LED lights from Lume Cube, Fire House Technology, and Stratus LEDs were tested on the M100 at a full battery charge with payload and performance parameters listed in Table 3.

Table 3. Comparison of different LED lights used.

Lighting System	Mass per light (g)	Lumen output per light	Beam Width (degrees)
Lume Cubes	99	1500	60
Fire House Technology	71	1600	100
Stratus LEDS	135	13000	60-160

Each lighting system was tested underground in the 895-102 drift at the Barrick Golden Sunlight Mine with no other light sources present. Using a *Dr. Meter LX1330B* light meter, the lux provided by each lighting system was measured at varying distances. A Leica laser distance measuring device was used to record the distance between the lights and the light meter positioned at the rock face. The Lume Cubes and Fire House Technology lights were measured at the highest brightness settings and two at a time to simulate use on the M100. The Stratus LEDs light was tested by itself, first with the parabolic reflector mounted and then with it removed. The results of the lighting experiment are displayed in Table 4 and Figure 4.

Table 4. Measured lux of each lighting system at various distances underground using a *Dr. Meter LX1330B* light meter.

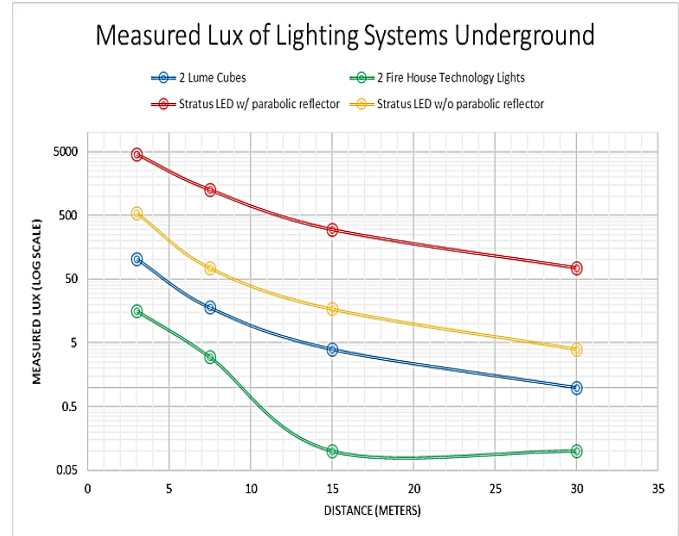| Distance at which lux was measured [m (ft.)]	Lighting System (number of lights) and Measured Lux			
	Lume Cubes (2)	Fire House Tech. (2)	Stratus LEDs w/ reflector (1)	Stratus LEDs w/o reflector (1)
3 m (10 ft.)	105	16	4500	550
7.5 m (25 ft.)	18	3	1250	75
15 m (50 ft.)	4	0.1	300	17
30 m (100 ft.)	1	0.1	75	4

Fig. 4. Comparison of the values of lux (lumens/m²) versus distance (m) for each lighting system.

Each of the light systems was tested on-board the M100 to determine if the illumination was sufficient for the Guidance VPS and for capturing RGB (red, blue, green) imagery. One set of lights was pointed toward the front of the aircraft for the benefit of capturing RGB imagery, and another set of lights was pointed downwards for the VPS system on the downward-facing Guidance sensor. When used with a parabolic reflector, the Stratus LEDs lighting system proved to be the only one that could illuminate the ground surface sufficiently for the Guidance VPS to work. When the parabolic reflector was removed from the Stratus LEDs lights, the M100 was able to use the Guidance VPS for positioning, but was limited to a flight ceiling of 6.7 m (22 ft.) before the aircraft became unstable. For frontward illumination, the Lume Cubes and Fire House Technology LEDs were found to have both limited ranges and narrow beam widths when compared to a Stratus LEDs light with the parabolic reflector removed, as observable in Tables 3 and 4. Weight became a limiting factor with all the lighting systems, and it became necessary to use a single 6S 3000mAh 25C LIPO battery (weight of 380 g) for 10 minutes of lighting using two Stratus LEDs lights.

6. THERMAL IMAGERY

Loose ground is an omnipresent hazard in many underground mines, and it can be subtle to the point of being undetectable to the human eye. National Institute of Occupational Safety and Health (NIOSH) researchers Iverson and Signer (2014) found that temperature differences as low as 0.2° C (0.36° F) captured with a thermal imager could be used to determine the location of loose ground. Their study evaluated the ability of thermal cameras to detect loose ground in six underground mines, and they found that warm, loose rock could be detected if the ventilation was cool. Underground ventilation can create a thermal contrast when cooler air decreases (or warmer air increases) the temperature of the loose rock relative to the in-situ rock temperature.

Rock masses at the Barrick Golden Sunlight Mine are either structurally massive breccia bodies, or thickly-bedded quartzites and sandstones. Deformation occurs along structural planes, and failure of the rock mass is rare. Water and clay are found along structures bounding the rock masses, and it was expected that these features would have cooler temperatures than intact rock.

Thermal imagery was analyzed and exported using FLIR ResearchIR, software that allows users to query the radiometric data embedded in the imagery. It was found that thermal images with narrow temperature ranges using gray scale defined the detail of images better than color scales, which typically had blurry textures. Figure 5 shows an example of imagery examined in ResearchIR, where warmer, loose rock is indicated by lighter colors and is outlined by a red polygon.

7. MODELING & ANALYSIS SOFTWARE

A variety of software was necessary for generating the 3D photogrammetry models from UAV imagery, analyzing and filtering the thermal images, and capturing geological structural data. With the purpose of identifying software that could accomplish these tasks, one important component of this research involved evaluating numerous software packages, including professional photogrammetry software that is typically used for terrestrial photogrammetry and capturing geological structural data. It was found that generating 3D point clouds and meshes from the UAV imagery captured underground was difficult due to changing lighting conditions, causing tie points to be generated with residual accuracies too large for the tolerances of the software. It is possible that the software could be used to accomplish all three tasks, but this will likely require more refinement of the underground, UAV-generated imagery and collaborative research with the software developers.

Lacking a one-software-fits-all solution, stand-alone photogrammetry products that can generate georeferenced, 3D models from still and video imagery, but cannot capture geological structural data, were evaluated. Of the photogrammetry software evaluated, Agisoft PhotoScan and Bentley ContextCapture consistently generated the most complete models and were not deterred by imagery with less than ideal quality. Agisoft PhotoScan was used for generating 3D models from still and video imagery with 50-80% overlap between pairs and was used to export 3D point-clouds. Bentley ContextCapture was used to generate 3D models from video imagery, where still frames are extracted from the video automatically at a user-defined time interval and used to generate the model. Figure 6 shows the geometry of the NEV stope composed of many still images extracted from a video in Bentley ContextCapture. The yellow, dashed line indicates the flight path of the M100, and the control points captured by the reflectorless total station and used to georeferenced the model are indicated by the yellow circles.
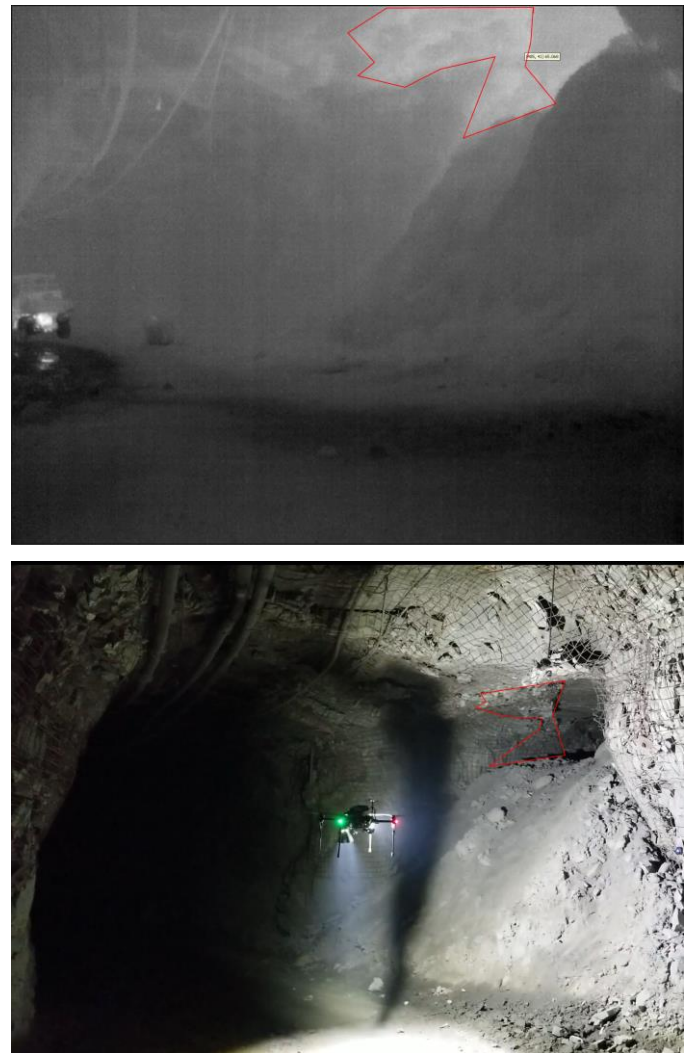

Fig. 5. Example of thermal imagery (top) and RGB imagery (bottom) in the 375 drift at the Golden Sunlight Mine. Warm air from a stope at a lower level is rising through the muck pile in the background. As a result, the loose ground outlined in red is warmer than the in-situ rock mass and shows up as a lighter color on the Zenmuse XT on the M100.
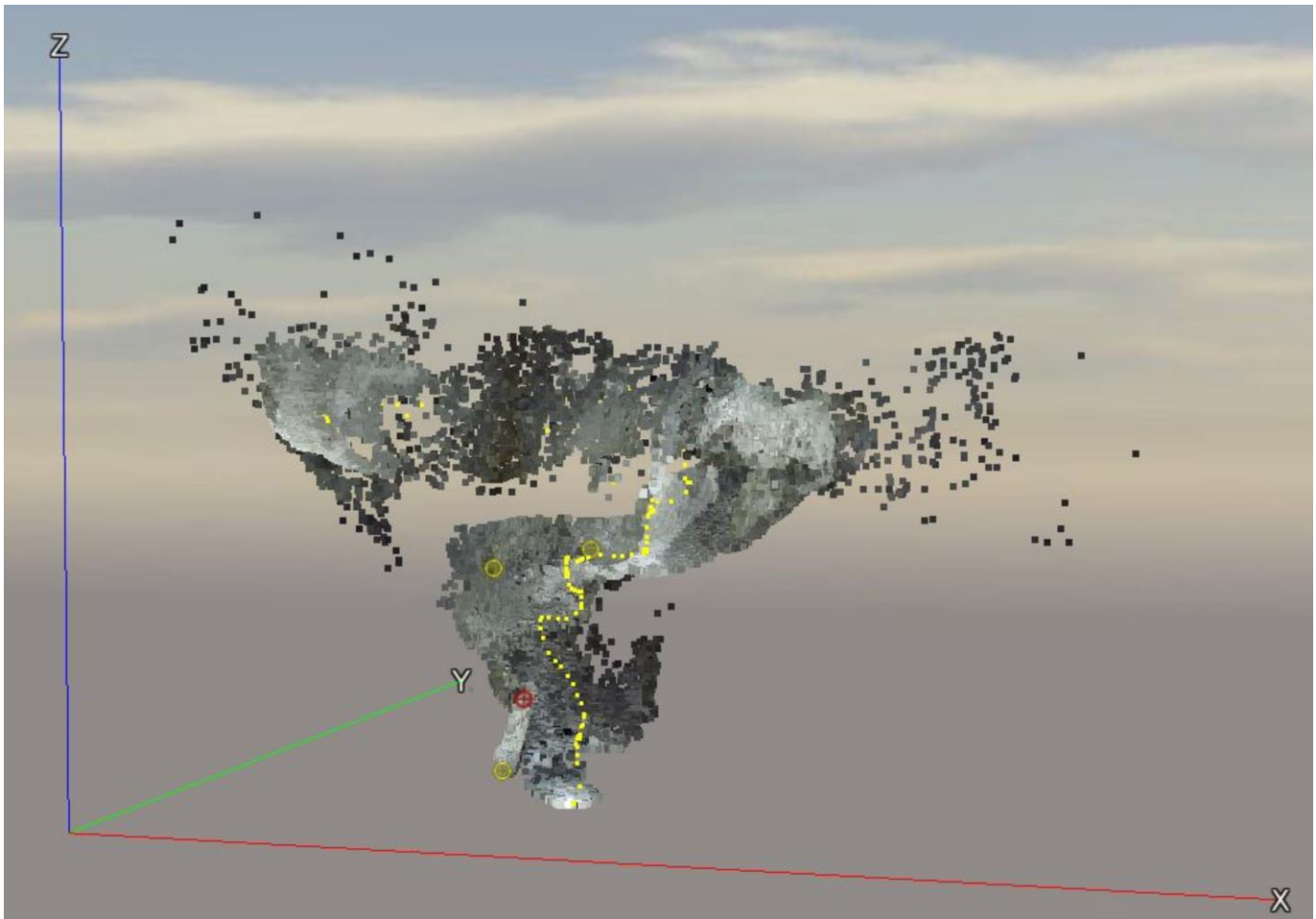
Fig. 6. Looking at a model of the 'NEV' stope at the Golden Sunlight mine produced using Bentley ContextCapture. The model shown is composed of individual photo stills from the video imagery. The flight-path of the M100 is indicated by the yellow, dashed line, and the control points are indicated by the yellow circles.

It is much more difficult to generate 3D models from thermal imagery as compared to RGB imagery. This is due to the lower resolution of thermal cameras (typically ranging from 60 x 40 pixels to 1280 x 1024 pixels) compared to that of digital cameras (typically ranging from 4000 x 3000 pixels to 6016 x 4008 pixels), and the limited number of match points generated when thermal images are merged for building photogrammetry models. With assistance from researcher Stephen Iverson at the NIOSH Spokane Research Center, success was achieved through draping the thermal images over a 3D photogrammetry model generated from RGB imagery. To do this, both RGB and thermal images of the same area are captured and imported into Agisoft PhotoScan, a 3D model using the RGB images is generated, tie points from common features in the RGB and thermal imagery are identified, and the tie points are used to merge the thermal imagery with the RGB model.

Geological structural data were interpreted using Split Engineering's Split-FX software. 3D point clouds generated in Agisoft PhotoScan and Bentley ContextCapture were imported into Split-FX and assigned RGB values from the point cloud metadata.

After each 3D point cloud is generated in Split-FX, a user-defined mesh is generated, which creates a 3D surface of the underground opening. Using the mesh, there is a function that allows for 'patches' (discontinuities) to be automatically or manually captured based upon the quantity of mesh triangles and relative position of triangles that make up a structural surface. Users are also able to capture the orientations of structures that show up as traces, which is an advantage of using data generated by photogrammetry, rather than LiDAR (Light Detection and Ranging). LiDAR data often does not utilize RBG data underground and instead assigns the same color to each point. Structures that are defined by traces may not be captured if they cannot be visually inferred from the 3D point cloud. After capturing the structural data, the user can then export this data into relevant kinematic analyses or numerical models.

8. PRELIMINARY TESTS OF THE SYSTEM

Initial tests of the flight capabilities of the DJI M100 and the proximity sensing capabilities of the DJI Guidance were conducted at the Montana Tech campus. To simulate the underground mining environment, indoor facilities that had low-light conditions, high magnetic interference,

and no GPS coverage were selected for test flights. Maintenance bays and racquetball courts, being very tall but not relatively wide, make ideal analogs for stopes; other flights were conducted in secured hallways and in the gymnasium (Figs. 7, 8 and 9).
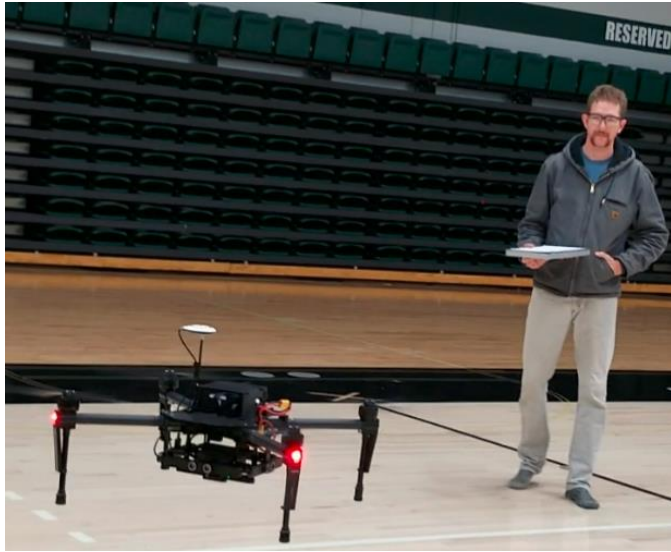

Fig. 7. The M100 undergoing initial flights at the Montana Tech gymnasium.

Fig. 8. An obstacle detection test for the Guidance system is shown in a maintenance bay at Montana Tech. In this instance, the Guidance is preventing the M100 from colliding with the wall.
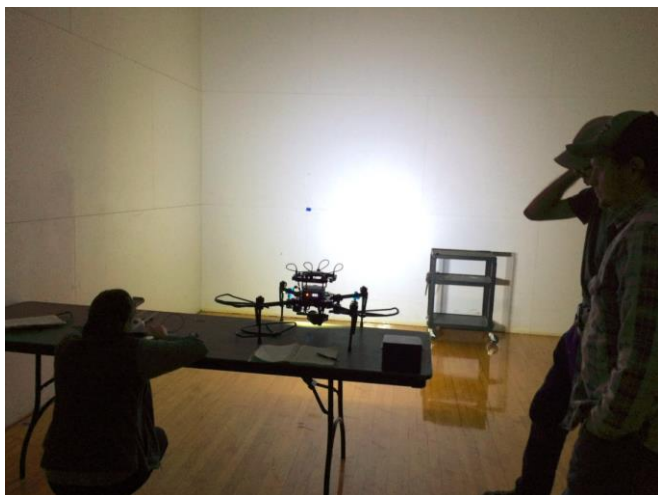
Fig. 9. An example of a test on the M100's on-board lighting and camera systems in a racquetball court at Montana Tech.

The capabilities of the M100's Guidance system, payload limits, and available flight modes were tested over the course of 4 months. After systematically adjusting the location of the sensors and repeating calibrations, the Guidance was successfully tested in a GPS-denied environment without ambient lighting (Fig. 8). Various components such as lights and cameras were mounted to the M100 to test its payload capacity and flight times. The M100 can be flown in three different flight modes: P-mode (positioning); A-mode (attitude); and K-mode (function). P-mode utilizes both GPS (when available) and the Guidance system to allow the M100 to hover stably and detect obstacles. A-mode is a free-flight mode that only accepts inputs from the pilot, and it disregards any on-board instruments. K-mode only uses on-board instruments, such as the Guidance. Of the modes tested, P-mode allowed the M100 to be more stable and fly without drifting, proving it to be the best choice for use with the Guidance system (DJI, March 2016).

9. UNDERGROUND FLIGHTS & RESULTS

Underground flights with the M100 system have been conducted at the Barrick Golden Sunlight Mine since December, 2017. To date, six site visits with successful flights have been logged in several different drifts and intersections, and in one stope.

9.1. Flight Procedure

Flights conducted underground at the Barrick Golden Sunlight Mine followed these steps:

1. A heading inspection was completed, and 5-point safety cards were reviewed. Scaling bars were used to remove any hazardous loose material around the draw point. Loose rocks on the sill were removed to create a level landing area.

2. A paintball marker was used to establish ground control points in the stope and around the draw point (Fig. 10).

3. After using 2 survey control points to resection a total station, the coordinates of the paintball marks were captured using reflectorless measurements (Fig. 11).

4. The drone and lights were assembled and tested before flight. (Note: Due to either temperature contrasts or high humidity, condensation develops on all the gear, including on the lenses of cameras. Good practice for future excursions is to allow the equipment to equilibrate with ambient temperature before flying.)

5. The drone was briefly flown in the stope access drift to ensure that everything was working properly. This was a critical step.

6. The drone was flown into the stope through the draw point. The pilot used the live-feed from the camera to navigate, while spotters helped to track

the drone in the stope by watching the beams of the on-board lighting move (Fig. 12).

7. The drone was flown back into the draw point, and footage from the micro SD card on the camera was used for generating models.

Fig. 10. Example of paintball marker in use for establishing control points. It was necessary to shoot multiple times at a single point because of dust on the ribs of the stopes and drifts.

Fig. 11. Total station set up at the entrance to the 'NEV' stope on the 4305 level. The total station had to be within line-of-sight of the survey control points and paintball marks within the stope.

Fig. 12. Still-image from a video captured by the M100 within the 'NEV' stope at the Barrick Golden Sunlight Mine. This image is looking NE along the long-axis of the stope from above the first draw point on the 4305 level. The approximate width of the stope is 10.5 m (35 ft.).

9.2. Underground RGB Flights

The M100 was flown underground at the Barrick Golden Sunlight mine in drifts and stopes that were not being actively mined at the time. Initial flights in drifts tested the abilities of the Guidance and various lighting systems, as well as the ability of the captured imagery to be used for generating models. After multiple flights indicated that payload and lighting systems were sufficient, the decision was made to test the capabilities of the M100 in a stope. The 'NEV' stope was selected because it had three draw points to choose from, was between blast and muck cycles, and contained muck piles angled toward the draw points that could potentially allow for recovery of the M100 if it crashed. The stope was 6 m (20 ft.) wide, 50 m (150 ft.) tall, and 120 m (400 ft.) long. The first flight in the stope captured imagery to the east, west, and above the first draw point (see Fig. 6). When the UAV flew east beyond the line-of-sight (LOS) of the remote controller, contact with the aircraft and flight control was lost. The pilot moved to a better vantage point at the draw point and regained control, confirming that flying outside LOS with the M100 was not an option with the current equipment. The M100 was then flown above the draw point, where its propellers displaced a large amount of dust. The dust blinded the forward-facing VPS on the Guidance, which resulted in the UAV flying towards the rib and crashing. The M100 was recovered and repaired after the crash.

Video imagery was used to generate 3D tile models of the stope in Bentley ContextCapture (Fig. 13) and Agisoft PhotoScan (Fig. 14). The tile models were exported as 3D point clouds into Split-FX, and structural data were digitized from the models (Fig. 15).
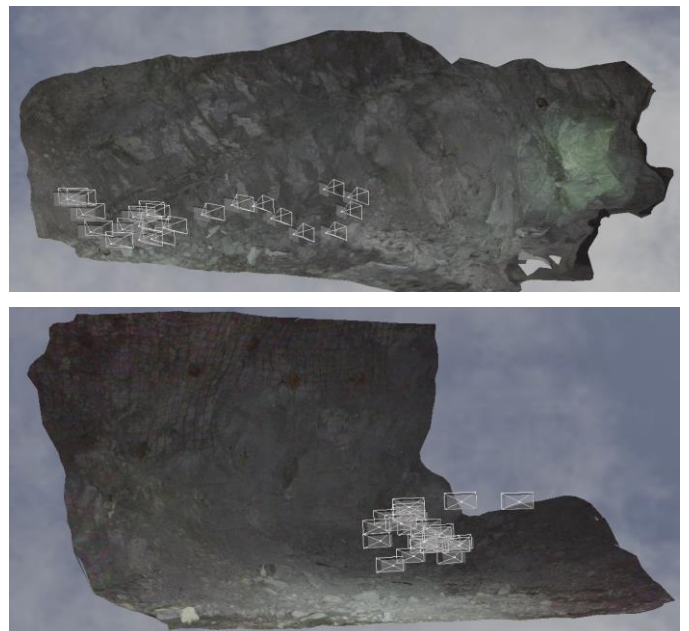

Fig. 13. 3D mesh of the S rib (top) and the N rib (bottom) of the 895-102 intersection at the Barrick Golden Sunlight Mine produced using Bentley ContextCapture from a video captured by a DJI M100. The gray boxes indicate the camera stations of the M100 while it was flying. On-board lighting was used.
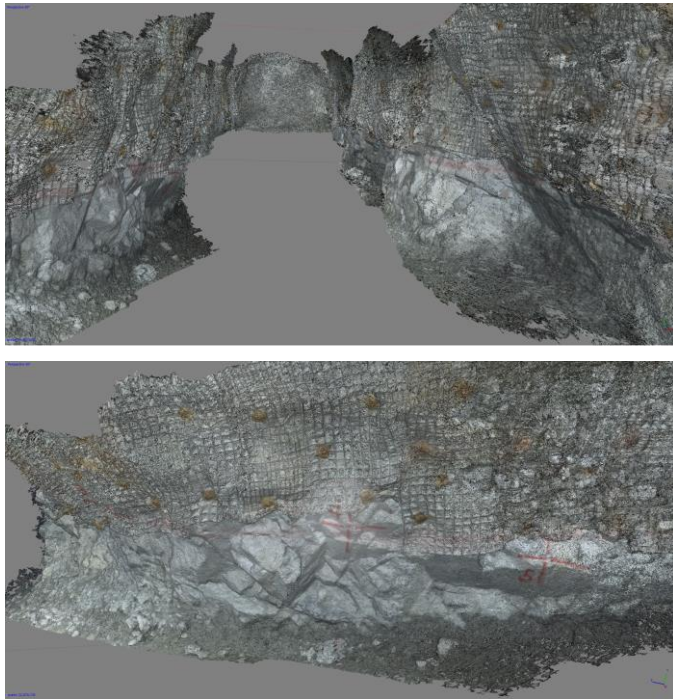
Fig. 14. 3D mesh of the 895-102 drift (top) and the N rib (bottom) of the 895-102 at the Barrick Golden Sunlight Mine produced using Agisoft PhotoScan from a video captured by a DJI M100. On-board lighting was used and the UAV was flown sideways with the camera facing toward the rib.

9.3. Underground Thermal Flights

After the M100 was successfully flown with the Zenmuse X3 (RGB) camera, the Zenmuse XT (thermal) camera was tested at Barrick Golden Sunlight in a drift because all of the stopes were actively being mined. Flights were conducted in the 375 drift, which has an exposure of the West Shear fault and loose rock contained by welded wire mesh. Ventilation was active in the drift, and using a *Pyle PMA90* anemometer, the dry bulb air temperature was found to be 19.8-20.3° C (67.6-68.5° F). Using a *Craftsman 50455* infrared thermometer, the temperatures of the rock mass and loose rock were found to be 15.7-15.8° C (60.3-60.4° F) and 15.6-15.7° C (60.1-60.3° F) respectively. Magnetic strobe lights fixed to friction bolts were used as georeferencing points because they are observable in the RGB imagery and as hot spots in the thermal imagery. Fig. 16 shows an example of loose ground (dark is warm) found above a muck pile and a magnetic strobe light.

Video imagery from the Zenmuse XT and Zenmuse X3 was used to generate 3D point clouds of the 375 drift in Agisoft PhotoScan. Three-dimensional point clouds generated using just the thermal imagery were difficult to interpret because points were typically monotone in color, and the software had difficulty in matching points when no reference points were established. Instead, the RGB imagery was used to generate the 3D point cloud, and thermal images were used in 2D form to verify if loose ground and dilated structures were present (Fig. 17). The West Shear fault was detected by the Zenmuse XT in

flight, because its damp clay infill was found to have a cooler temperature (14.7° C/ 57.7° F) than the surrounding rock, and it shows up as a dark lineation on the thermal imagery (Fig. 17, bottom image).
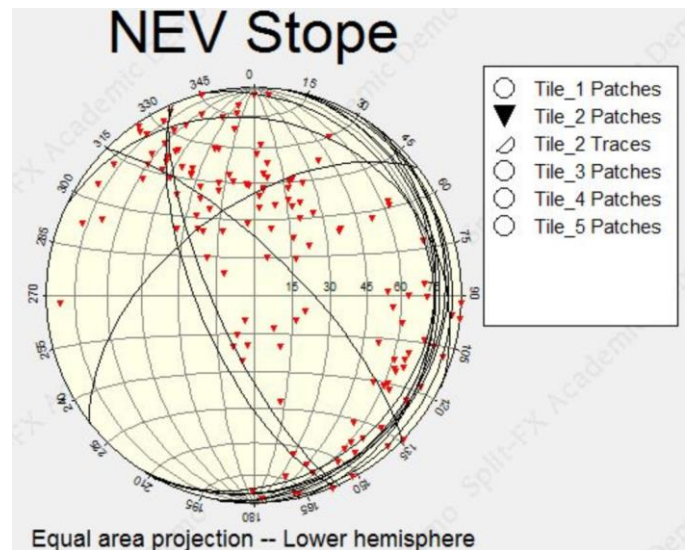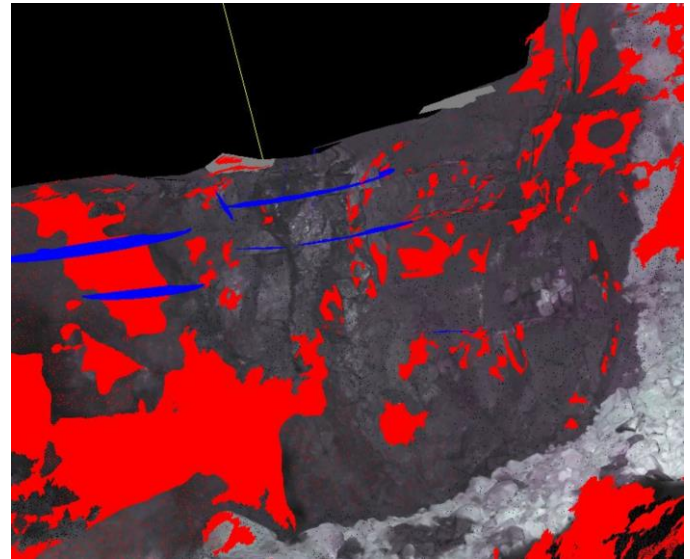

Fig. 15. Geological structures (red discontinuity planes and blue traces) in the NEV stope are identified using Split-FX (top). Structures digitized from the 3D point cloud are shown in a lower hemisphere stereonet in Split-FX (bottom).
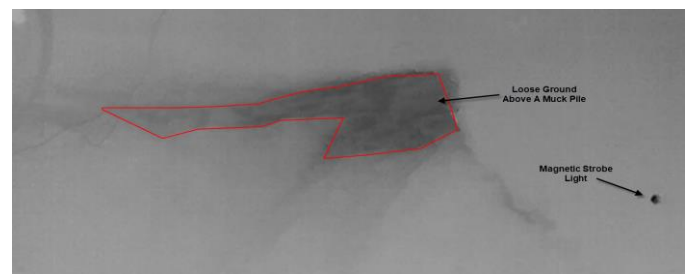

Fig. 16. A thermal still from a video recorded with the Zenmuse XT on the M100 while flying in the 375 drift. Warm material is indicated by darker colors, and loose ground (outlined in red) can be observed above the muck pile. The loose rock had temperatures up to 18.6° C (65.4° F), while the intact rock around it had temperatures up to 17.2° C (63° F). A magnetic strobe light was used as a reference point.
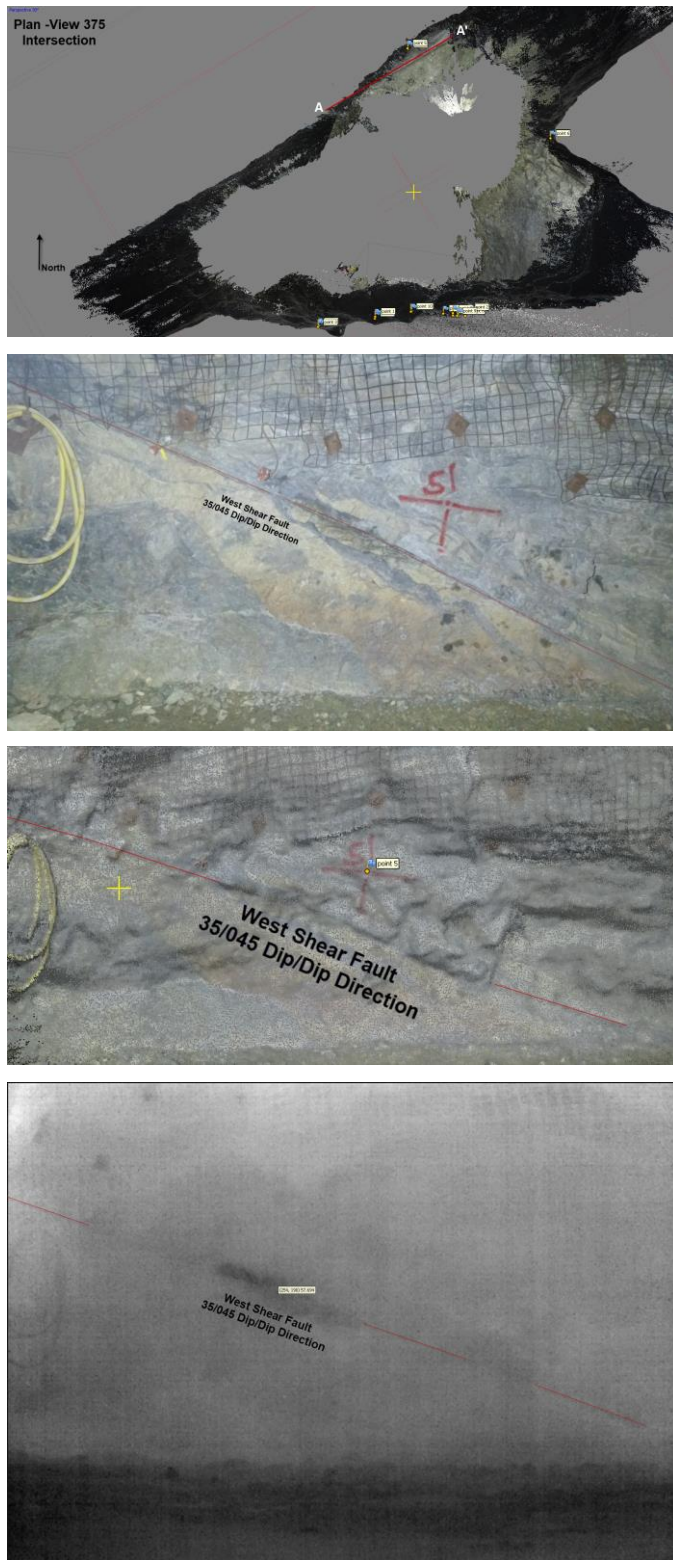
Fig. 17. The top image shows a plan-view of a 3D point cloud generated from RGB imagery for the 375 intersection. The red section line indicates the location and orientation of the lower images. The lower three images are looking north at an exposure of the West Shear fault with RGB (second from top), 3D point cloud (second from bottom), and thermal (bottom) imagery from two separate flights by the M100. The fault is a basal release plane for a global instability at the mine, and typically has damp to wet montmorillonite as infill. In the thermal imagery, the clay is cooler (14.7° C/ 57.7° F) than the surrounding rock and is indicated by a dark lineation.

10. SUMMARY & CONCLUSIONS

Successful flights underground at the Barrick Golden Sunlight Mine, the generation of 3D models from UAV-captured imagery, and the identification of geological data from photogrammetry models confirm that the off-the-shelf technologies used in this study can be effectively combined to serve as a geotechnical tool in the underground mining environment. Thermal imagery lacks the refinement and point density of RGB models, but has the potential to be invaluable for detecting loose ground and dilated structures with infill when compared with RGB imagery. Future plans include flights in stopes with the RGB and thermal cameras, refining the 3D RGB and thermal models, and testing a new aerial platform that can carry both cameras at the same time.

New technologies utilizing SLAM (simultaneous localization and mapping), LiDAR, and autonomous functions have been developed to allow for more complete high-quality data to be captured, but costs are currently much higher than the tools used in this study. With time, as costs decrease and experience increases, the use of UAV-captured imagery will become more widespread.

11. ACKNOWLEDGEMENTS

REFERENCES

1. DJI, 2015. *Guidance User Manual*. Version 1.6, 21-22. Shenzhen, PRC

2. DJI, March 2016. *DJI M100 User Manual*. Version 1.6, 59, 72. Shenzhen, PRC

3. DJI, May 2016. *Zenmuse XT User Manual*, Version 1.2, 17-18. Shenzhen, PRC

4. FLIR, 2016. *User's Manual FLIR Cx Series*, FLIR Systems, Inc. Wilsonville, OR

5. Iverson, S. and S. Signer, 2014. Assessment and Detection of Loose Rock Hazards in Underground Metal Mines Using Thermal Imaging. *2014 SME Annual Meeting & Exhibit (SME 2014): Leadership in Uncertain Times, Salt Lake City, 23-26 February 2014*.: Society for Mining, Metallurgy, and Exploration, Inc., 2014 July; 666-672. Englewood, CO.

6. Knight, R., 2016. Monitoring, Mapping, Measuring: How Drones Are Changing the Mining Industry. *Inside Unmanned Systems: Engineering, Policy, and Practice.* Autonomous Media, LLC. http://insideunmannedsystems.com/monitoring-mapping-measuring-drones-changing-mining-industry/